ogy between these craters and the developed criteria were attributed to a diameter effect, which is now being studied.

Concluding Remarks

This study has indicated that the following four criteria can be used to identify and distinguish meteoroid impacts from low-energy impact damage in fused silica: 1) the ratio of average surface diameter to the depth of the deepest fissure, 2) the percentage of the total surface area blacked-out because of total reflection, 3) the cross-sectional profile, and 4) the surface characteristics. By detailed examination of the features of craters in fused silica, one can estimate the velocity at which it was struck.

Additional studies must be performed to determine the extent to which projectile diameter and density affect the cited criteria. More data are needed in the 1.0–6.0 km/sec range, as well as at velocities in excess of 10 km/sec. Techniques must be developed to launch identical projectiles at all velocity ranges.

References

[1] Naumann, R. J., "The Near Earth Meteoroid Environment," TN D-3717, Nov. 1966, NASA.

[2] Gault, D. E. and Moore, H. J., "Scaling Relationships for Microscale to Megascale Impact Craters," TMX-54996, Feb. 1965, NASA.

MARCH 1970 J. SPACECRAFT VOL. 7, NO. 3

Stresses and Deformations in Melting Plates

EDWARD FRIEDMAN*
General Electric Company, Philadelphia, Pa.

AND

BRUNO A. BOLEY†
Cornell University, Ithaca, N. Y.

The temperature, stresses, and deformations in a melting plate are calculated. The temperature solution is obtained by means of repeated use of the concept of penetration depth with the heat balance approach. Its accuracy is measured by comparison with the results of several other solution methods. Approximate, explicit solutions for melt thickness and penetration depth are included to facilitate rapid calculations. The mechanical response is derived considering the material to be elastic-perfectly plastic with a temperature-dependent yield stress decreasing linearly to zero at the melting temperature. For a plate free of mechanical loading, elastically computed deformations are found to be fairly good upper-bound solutions to those calculated including plasticity effects. An approximate method of solution is presented for the determination of the mechanical response after peak loading is attained. The phenomenon of plastic collapse of an edge-loaded melting plate is illustrated in a sample problem.

Introduction

WHILE considerable work has been done in recent years on the calculation of melting rates and temperature distributions in melting and ablation problems,‡ comparatively little effort has been expended on analyses of the resulting thermal stresses and deformations. The investigations that have thus far been carried out in this direction include the work of Rogers and Lee,[4] concerning the viscoelastic behavior of an ablating sphere of polymethol methacrylate, Sternberg and Gurtin's[5] corresponding proof of uniqueness of solution, Weiner and Boley's[6] elastoplastic solution for stresses in a solidifying slab, Schuyler and Friedman's[7] elastoplastic treatment of an ablating heat shield structure, and Tadjbakhsh's[8] elastic dynamic analysis of the stresses in a half-space with a moving boundary. Numerous papers have been written on hollow viscoelastic cylinders with eroding inner boundaries, which relate to solid-propellant rocket motors, but thermal effects have generally been neglected.

This paper presents a general approximate method for the determination of temperatures, stresses and deformations in a melting plate. Though the design of such plates has in the past been based mainly on their primary function as heat sinks, and has, therefore, generally neglected the mechanical aspects, certain questions arise that may become important with increasing sophistication of design. Among these questions are the failure or cracking of the ablating layer, the influence of structural deformations on the aerodynamic characteristics, the possibility of using the ablating member as a part of the primary load-carrying structure, and even the eventuality of its possible repeated use in more than one mission. Clearly such matters cannot be treated without reference to the mechanical response, a treatment of which indeed forms the primary purpose of the present paper.

In order to determine an analytical solution for stresses and deformations in an ablating plate, it is first necessary to establish the temperature distribution. This is done by an approximate method, although, of course, numerous solutions of this part of the problem have appeared in the literature. The approach selected here is novel in that it repeatedly

Received July 28, 1969; revision received October 31, 1969. The results in this paper are based in part on a dissertation submitted to Columbia University. The research was sponsored by the Office of Naval Research.

* Research Engineer, Solid Mechanics Laboratory, Re-entry & Environmental Systems Division. Associate Fellow AIAA.

† Joseph P. Ripley Professor of Engineering, Department of Theoretical and Applied Mechanics.

‡ Complete bibliographies and surveys may be found in Refs. 1–3. The latter is an exposition of integral methods of analysis, which form the basis of the method employed for the temperature solution in this paper.

employs the penetration depth concept in order to simulate the effect of any new surface disturbance (e.g., start of melting). In this way, accurate results are obtained not only for the growth of the melt thickness, but also for the entire temperature distribution, which is an essential requirement if accurate stresses and deformations are to be found. Also necessary for the ease of calculation of the mechanical response is the fact that this method (in common with the other approximate approaches) yields results in a simple analytical form; however, the present temperature solutions also exhibit a smooth transition between the premelting and postmelting regimes (i.e., continuous time derivatives of temperature throughout the body at the time of start of melting—a condition not generally satisfied by existing approximate analytical solutions), and thus are in good agreement with exact short-time solutions.

Upon completion of the thermal solution, the calculation of the stresses and deformations is carried out on the basis of the assumption that the material is an elastic-perfectly plastic one, but with a temperature-dependent yield stress Y. More precisely, it is assumed that Y decreases linearly from a value Y_0 at base temperature T_0, to zero at the melting temperature T_m. Though this assumption may be somewhat of an oversimplification for typical re-entry materials, it is adequate for the purposes of this paper, since it is generally valid for $(T_m + T_0)/2 < T < T_m$—the temperature range of primary concern. Thus,

$$Y(T) = Y_0(T_m - T)/(T_m - T_0) \text{ for } T \geq T_0 \qquad (1)$$

The von Mises yield criterion is employed, or[9]

$$f(S_{ij}, T) = \tfrac{1}{2}S_{ij}S_{ij} - \tfrac{1}{3}[Y(T)]^2 = 0 \qquad (2)$$

where the $S_{ij} = \sigma_{ij} - \tfrac{1}{3}\sigma_{kk}\delta_{ij}$ represent the components of the stress deviator.

The problem considered is that of a plate, whose geometry is shown in Fig. 1.§ The resulting heat flow is one-dimensional across the plate thickness; thus, the temperature T satisfies (with thermomechanical coupling neglected and under the assumption of constant thermal properties) the equation

$$\kappa\partial^2T/\partial x^2 - \partial T/\partial t = 0 \qquad (3)$$

where κ is the thermal diffusivity. The heat input $Q(t)$ is taken to vary with time as a square pulse, namely,

$$Q(t) = \begin{cases} 0 & t < 0 \\ Q_0 & 0 < t < t^* \\ 0 & t^* < t \end{cases} \qquad (4)$$

The constants Q_0 and t^* can be adjusted so as to simulate conditions encountered during atmospheric re-entry. The ablated layer is assumed to be instantaneously removed. This assumption provides a good approximation to the problem of an ablating solid under certain conditions of aerodynamic heating, as discussed, for example, in Refs. 10–15.

In developing numerical results, it was borne in mind at all times that it was desired to develop an accurate but approximate approach and, for this reason, several simplifications of the problem were investigated and their accuracy was assessed. In the temperature solution, the principal simplifications are purely numerical, and involve the dimensionless melt thickness $S(\tau)$ and the use of the function $F(\tau)$ to obtain $\dot{S}(\tau)$. In the stress and deformation solution the assumption of simultaneous elastic unloading is found acceptable. The permissibility of calculating deflections (but not stresses) purely elastically (i.e., the validity of the "strain-invariance principle"[16,17]) is examined.

§ The plate is taken to be circular for the calculation of stresses and deformations, but can be of arbitrary shape in the thermal analysis.

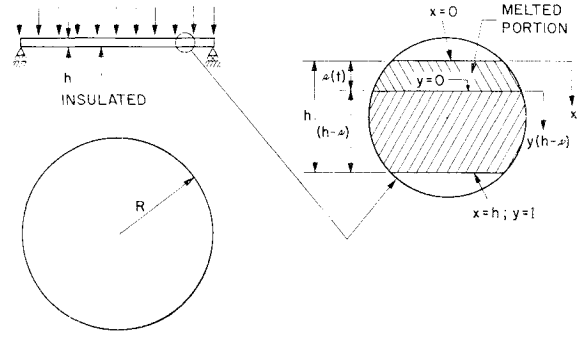

Fig. 1 Geometry of plate.

The present paper does not include, for the sake of brevity, all details of the calculations, but only the equations essential to an understanding of the solution and of the physical character of the results. Full details may be found in Ref. 18.

Temperature Calculation

The analysis presented here employs the heat-balance integral and makes repeated use of the concept of penetration depth, introduced by Biot.[19] Three different penetration depths are employed, each of which represents the depth of penetration of a disturbance originating at the heated surface, and appearing mathematically as a change in the boundary conditions. Beyond this depth, heating of the plate is unaffected by the particular surface phenomenon. The three surface phenomena to be considered are: application of the heat pulse, onset of melting, and removal of the heat pulse, occurring at times $t = 0$, $t = t_m$, and $t = t^*$, respectively; they give rise to the penetration depths q_0, q_1, and q_2, respectively. The form of the temperature solution depends on the relative magnitudes of the various penetration depths, which in turn depend on the magnitude of the heat input, as will subsequently be shown. The accuracy of the solution depends, of course, on the form taken for the temperature distribution.

The temperature satisfies the Fourier heat-conduction Eq. (3) in the region $s(t) < x < h$, where $s(t)$ is the melt thickness. Define the dimensionless variables:

$$\theta = \frac{T}{T_m}; \quad y = \frac{x - s(t)}{h - s(t)}; \quad \tau = \frac{\kappa(t - t_m)}{h^2} = \frac{\kappa t}{h^2} - \tau_m \qquad (5)$$

$$S(\tau) = s(t)/h$$

where T_m is the melting temperature, and $\tau_m = \kappa t_m/h^2$. Upon transformation to dimensionless variables, it is found that

$$\partial/\partial t = (\kappa/h^2)\{\partial/\partial\tau - [(1 - y)\dot{S}/(1 - S)]\partial/\partial y\}$$

and

$$\partial^2/\partial x^2 = \{1/[h^2(1 - S)^2]\}\partial^2/\partial y^2$$

Equation 3 thus becomes

$$\partial^2\theta/\partial y^2 - (1 - S)^2\partial\theta/\partial\tau + \dot{S}(1 - S)(1 - y)\partial\theta/\partial y = 0; \qquad (6)$$

$$0 < y < 1; \quad \tau > -\tau_m$$

The boundary and initial conditions, both in dimensional and dimensionless form, are as follows:

$$T = T_m \text{ on } x = s(t), t > t_m; \ \theta = 1 \text{ on } y = 0, \tau > 0 \qquad (7a)$$

$$\kappa\frac{\partial T}{\partial x} = -Q(t) + \rho l\frac{ds}{dt} \text{ on } x = s(t), t > 0$$

$$\frac{\partial\theta}{\partial y} = -2\bar{Q}(1 - S)\left(1 - \frac{\dot{S}}{2\bar{Q}\mu}\right) \text{ on } y = 0, \tau > -\tau_m \qquad (7b)$$

Table 1 Melt thickness and penetration depth in melting range

Heating rate	Time period	Equations for $S(\tau)$ and $q_1(\tau)$	Approximate expressions for $S(\tau)$ and $F(\tau)$	
$0 < \bar{Q} < 1$	$0 \le \tau \le \tau_{q_1=1}$	$3\frac{S}{\bar{Q}\mu} + [3 - 2(1-S)](1-2\tau) - (1-S)(1-q_1) \times [1 - 2\tau - (1-S)^2] - 1 = 0$ $(1-S)^2 + \frac{1-2\tau-(1-S)^2}{q_1} = (1-S)\left(1 - \frac{\dot{S}}{2\bar{Q}\mu}\right)$	$S = (\tau/\tau_h)^n$	$F = 1 - 2\tau$
			$\tau_h = \frac{1}{3} + \frac{1}{2\bar{Q}\mu}$	$F = \frac{1}{2}\left(\frac{\tau_h - \tau}{\tau_h - \tau_{q_1=1}}\right)^m$
	$\tau_{q_1=1} \le \tau \le \tau^*$	$3\frac{S}{\bar{Q}\mu} + 3(1-2\tau) - 2(1-S)^2\left(1 - \frac{\dot{S}}{2\bar{Q}\mu}\right) - 1 = 0$	$n = \frac{3}{2}\frac{\bar{Q}\mu}{\bar{Q}\mu + 1} + 1$	$m = \frac{3 + \bar{Q}\mu}{2\bar{Q}\mu}$
$1 < \bar{Q} < 2^a$	$0 \le \tau \le \tau_{q_0=1}$	$3\frac{S}{\bar{Q}\mu} + 3\left[1 - 2\tau - \frac{2\bar{Q}^2 - 3\bar{Q} + 1}{3\bar{Q}^2}\right] - \frac{2}{\bar{Q}}(1-S) - (1-S) \times (1-q_1)\left[\frac{1}{\bar{Q}} - \frac{q_0^2(1-S)^2}{1-(1-q_0)(1-S)}\right] - (1-S)(1-q_0) \times \frac{q_0^2(1-S)^2}{1-(1-q_0)(1-S)} - 1 = 0$ $\frac{1}{q_0}\left[\frac{q_0^2(1-S)^2}{1-(1-q_0)(1-S)}\right] + \frac{1}{q_1}\left[\frac{1}{\bar{Q}} - \frac{q_0^2(1-S)^2}{1-(1-q_0)(1-S)}\right] = (1-S)\left(1 - \frac{\dot{S}}{2\bar{Q}\mu}\right)$ $q_0 = \frac{[6(\tau+\tau_m)]^{1/2} - S}{1-S}; \quad \tau_m = \frac{1}{6\bar{Q}^2}$		$F = 1 + \frac{6\bar{Q}^2\tau}{\bar{Q}^2 - 6\bar{Q} + 2}$
	$\tau_{q_0=1} \le \tau \le \tau_{q_1=1}$	$3\frac{S}{\bar{Q}\mu} + [3 - 2(1-S)]\left[1 - 2\tau - \frac{2\bar{Q}^2 - 3\bar{Q} + 1}{3\bar{Q}^2}\right] - (1-S) \times (1-q_1)\left[1 - 2\tau - (1-S)^2 - \frac{2\bar{Q}^2 - 3\bar{Q} + 1}{3\bar{Q}^2}\right] - 1 = 0$ $(1-S)^2 + \frac{1}{q_1}\left[1 - 2\tau - (1-S)^2 - \frac{2\bar{Q}^2 - 3\bar{Q} + 1}{3\bar{Q}^2}\right] = (1-S)\left(1 - \frac{\dot{S}}{2\bar{Q}\mu}\right)$	$S = (\tau/\tau_h)^n$ $\tau_h = \frac{3\bar{Q} - 1}{6\bar{Q}^2} + \frac{1}{2\bar{Q}\mu}$ $n = \frac{6\bar{Q}\mu}{(11\bar{Q} - 7)(\bar{Q}\mu + 1)} + 1$	
	$\tau_{q_1=1} \le \tau \le \tau^*$	$3\frac{S}{\bar{Q}\mu} + 3\left[1 - 2\tau - \frac{2\bar{Q}^2 - 3\bar{Q} + 1}{3\bar{Q}^2}\right] - (1-S)^2 \times \left(1 - \frac{\dot{S}}{2\bar{Q}\mu}\right) - 1 = 0$		$F = \frac{1}{2}\left(\frac{\tau_h - \tau}{\tau_h - \tau_{q_1=1}}\right)^m$ $m = \frac{3 + \bar{Q}\mu}{2\bar{Q}\mu}$
$\bar{Q} > 2^a$	$0 \le \tau \le \tau_E$	(Same as $1 < \bar{Q} < 2$ in $0 \le \tau \le \tau_{q_0=1}$)		
	$\tau_E \le \tau \le \tau_{q_1=1}$	$3\frac{S}{\bar{Q}\mu} + 3\left[1 - 2\tau - \frac{2\bar{Q}^2 - 3\bar{Q} + 1}{3\bar{Q}^2}\right] - \frac{2}{\bar{Q}}(1-S) - (1-S)(1-q_1)\frac{1}{\bar{Q}} - 1 = 0$ $\frac{1}{q_1\bar{Q}} = (1-S)\left(1 - \frac{\dot{S}}{2\bar{Q}\mu}\right)$		$F = 1 - 2\bar{Q}\tau$
	$\tau_{q_1=1} \le \tau \le \tau^*$	(Same as $1 < \bar{Q} < 2$ in $\tau_{q_1=1} \le \tau \le \tau^*$)		$F = \frac{1}{\bar{Q}}\left(\frac{\tau_h - \tau}{\tau_h - \tau_{q_1=1}}\right)^m$ $m = \frac{3 + \bar{Q}\mu}{2\bar{Q}\mu}$

[a] For large μ; for smaller values of μ, this limiting value of $\bar{Q}$ is greater than 2.

$$\frac{\partial T}{\partial x} = 0 \text{ on } x = h, t > 0; \frac{\partial \theta}{\partial y} = 0 \text{ on } y = 1, \tau > -\tau_m \quad (7c)$$

$$T = T_0, 0 < x < h, t = 0; \theta = 0, 0 < y < 1, \tau = -\tau_m \quad (7d)$$

$$s \equiv 0, 0 < t \le t_m; S \equiv 0, -\tau_m < \tau \le 0 \quad (7e)$$

where dots indicate differentiation with respect to τ, and the two dimensionless parameters:

$$\bar{Q} = Q_0 h/(2kT_m); \quad \mu = cT_m/l \quad (8)$$

have been introduced, where k is the thermal conductivity, c the specific heat, and l the latent heat of melting. The further notation

$$F(\tau) = (1-S)[1 - \dot{S}/(2\bar{Q}\mu)] \quad (9)$$

will be found convenient later.

For continuity of $\partial T/\partial x$ at $x = 0$ and $t = t_m$, and nonzero latent heat of melting,

$$(ds/dt)t_m = 0 \text{ or } \dot{S}(0) = 0 \quad (10)$$

If heating continues for a sufficient time, the plate will melt completely at $t = t_h(\tau = \tau_h)$, or $s(t_h) = h$. From Eq. (7b) and (7c), then,

$$(ds/dt)t_h = Q_0/(\rho l) \quad (11)$$

In dimensionless form this becomes

$$\dot{S}(\tau_h) = 2\bar{Q}\mu; \quad S(\tau_h) = 1 \quad (11a)$$

Integration of Eq. (6) over the thickness of the plate and use of the boundary conditions (7) result in

$$2\bar{Q} - \frac{1+\mu}{\mu}\dot{S} = \frac{d}{d\tau}\left[(1-S)\int_0^1 \theta(y,\tau)dy\right] \quad (12)$$

This equation represents an energy balance per unit area of the plate, and will be used in lieu of the heat conduction Eq. (6) in our approximate solution. Integration over time from $\tau = -\tau_m$ gives

$$2\bar{Q}(\tau + \tau_m) = \frac{1+\mu}{\mu} S(\tau) + [1 - S(\tau)] \int_0^1 \theta(y,\tau)dy \quad (13)$$

This equation represents the balance of energy accumulated from the time at which the heat pulse is initially applied, indicating that part of the total heat applied after melting goes toward overcoming the latent heat of melting, while the rest is used in heating the plate; it will henceforth be referred to as the overall heat balance. Prior to melting, Eq. (13) can be simplified by setting $S \equiv 0$. Further, the time of total melting—computed when $S(\tau) = 1$—is given as

$$\tau_h = (1 + \mu)/(2\bar{Q}\mu) - \tau_m \quad (14)$$

Premelting Solution

In the premelting regime ($-\tau_m < \tau < 0$), let

$$\theta(y,\tau) = \begin{cases} \bar{Q}q_0 (1 - y/q_0)^2 & 0 < y < q_0 \\ 0 & q_0 < y < 1 \end{cases} \quad (15)$$

Eq. (13), with $S = 0$, then gives

$$q_0 (\tau) = [6(\tau + \tau_m)]^{1/2} \quad (15a)$$

This solution satisfies Eqs. (7), insures continuity of the first spacial derivative of temperature throughout the body, and is valid until either $q_0 = 1$ or $\theta(0,\tau) = 1$, whichever occurs first. From the first of Eqs. (15) it is clear that the occurrence of one or the other of these possibilities will depend on whether $\bar{Q}$ is smaller or larger than unity. Thus, two cases arise, with $0 < \bar{Q} \leq 1$ and $\bar{Q} > 1$, respectively.

When $0 < \bar{Q} \leq 1$, Eqs. (15) are valid in $-\tau_m \leq \tau \leq \tau_{q_0=1}$, where $\tau_{q_0=1}$ is the time at which $q_0 = 1$. In the time range $\tau_{q_0=1} \leq \tau \leq 0$, we let

$$\theta(y,\tau) = 1 - \bar{Q}(1 - 2\tau) + \bar{Q}(1 - y)^2 \quad (16)$$

This solution satisfies the heat equation identically, as well as the start-of-melting condition $\theta(0,0) = 1$. It is easily seen that

$$\tau_{q_0=1} = -(1 - \bar{Q})/(2\bar{Q}) \text{ and } \tau_m = (3 - 2\bar{Q})/(6\bar{Q}) \quad (16a)$$

On the other hand, when $\bar{Q} > 1$, Eqs. (15) are valid in $-\tau_m \leq \tau \leq 0$. Eq. (15a) and the condition $\theta(0, 0) = 1$ then give

$$\tau_m = 1/(6\bar{Q}^2) \quad (17)$$

Postmelting Solution

Again, two cases arise. Consider first the heating range $0 < \bar{Q} \leq 1$. For short postmelting times, it is required that, beyond the penetration depth q_1, heating of the plate continue unaffected by the melting phenomenon. The temperature distribution is thus of the form

$$\theta(y,\tau) = \begin{cases} 1 - \bar{Q}(1 - 2\tau) + \bar{Q}(1 - S)^2(1 - y)^2 + \chi(y,\tau) & 0 < y < q_1 \\ 1 - \bar{Q}(1 - 2\tau) + \bar{Q}(1 - S)^2(1 - y)^2 & q_1 < y < 1 \end{cases} \quad (18)$$

where $q_1(0) = 0$. Note that the undisturbed region of the plate ($q_1 < y < 1$) has a temperature distribution, with respect to the dimensional thickness variable x, identical to that before melting [Eq. (16)]. Stipulating temperature and its spatial gradient to be continuous at all y, and satisfying Eq. (7a),

$$\chi(y,\tau) = \bar{Q}[1 - 2\tau - (1 - S)^2] \quad (19)$$

The unknowns $S(\tau)$ and $q_1(\tau)$ are found by the simultaneous solution of the two equations obtained by substituting Eqs. (18) and (19) into the overall heat balance equation (13) and the boundary condition (7b). These equations are presented in Table 1 and, of course, are valid only until the time at which $q_1 = 1$, denoted by $\tau_{q_1=1}$. For large values of $\bar{Q}\mu$, these equations yield

$$\tau_{q_1=1} = \tfrac{1}{4} \quad (20)$$

In the time range $\tau_{q_1=1} \leq \tau \leq \tau^*$, where τ^* is the time at which the heat pulse is removed (provided this occurs before complete melting), we let [see Eq. (9)]

$$\theta(y,\tau) = 1 - \bar{Q}F(\tau) + \bar{Q}F(\tau)(1 - y)^2 \quad (21)$$

This solution satisfies all three boundary conditions [Eqs. (7a, 7b, and 7c)]. The unknown $S(\tau)$ is found by solving the differential equation resulting from the substitution of Eq. (20) into the over-all heat balance equation (13), and given in Table 1.

Consider now the second case; i.e., $\bar{Q} > 1$. Since the heat penetration at the start of melting is not complete [$q_0(0) < 1$], a portion of the plate ($q_0 < y < 1$) remains at the initial temperature $\theta = 0$. Proceeding as in the previous case, the temperature solution is found to be

$$\theta(y,\tau) = \begin{cases} \bar{Q}\dfrac{q_0^2(1 - S)^2}{1 - (1 - q_0)(1 - S)}\left(1 - \dfrac{y}{q_0}\right)^2 + \psi(y,\tau) & 0 < y < q_1 \\ \bar{Q}\dfrac{q_0^2(1 - S)^2}{1 - (1 - q_0)(1 - S)}\left(1 - \dfrac{y}{q_0}\right)^2 & q_1 < y < q \\ 0 & q_0 < y < 1 \end{cases} \quad (22)$$

In the region $q_1 < y < 1$, the temperature solution is identical to that of Eq. (15) before melting. In terms of the dimensionless y variable, q_0 [Eq. (15a)] becomes

$$q_0(\tau) = \{[6(\tau + \tau_m)]^{1/2} - S(\tau)\}/[1 - S(\tau)] \quad (22a)$$

Continuity of θ and $\partial\theta/\partial y$ at all y and satisfaction of Eq. (7a), result in

$$\psi(y,\tau) = [1 - \bar{Q}q_0^2(1 - S)^2/\{1 - (1 - q_0)(1 - S)\}] \times (1 - y/q_1)^2 \quad (23)$$

Once again, $S(\tau)$ and $q_1(\tau)$ are found by the simultaneous solution of the two equations resulting from the substitution of Eqs. (22) and (23) into Eqs. (7b) and (13), and the use of Eq. (22a). These equations are given in Table 1, and are valid until either $q_0 = 1 (\tau = \tau_{q_0=1})$ or $q_1 = q_0 (\tau = \tau_E)$, whichever occurs first. It is easily shown from the equations for S, q_1, and q_0 that, for large values of μ, q_0 will completely penetrate the plate before q_1 if $1 < \bar{Q} < 2$. The two penetration depths will become coincident at $\tau = \tau_E$ if $\bar{Q} > 2$.¶ Two subcases are thus considered (i.e., $1 < \bar{Q} < 2$ and $\bar{Q} > 2$).

When $1 < \bar{Q} < 2$, Eqs. (22-23) are valid in $0 \leq \tau \leq \tau_{q_0=1}$. From Eqs. (17) and (22a), it is seen that

$$\tau_{q_0=1} = (\bar{Q}^2 - 1)/(6\bar{Q}) \quad (24)$$

Considering the time range $\tau_{q_0=1} \leq \tau \leq \tau_{q_1=1}$, a solution which is continuous with that of the previous time range at $\tau = \tau_{q_0=1}$, and satisfies boundary conditions (7a) and (7c) is as

¶ For lower values of μ, this limiting value of $\bar{Q}$ will be greater than 2.

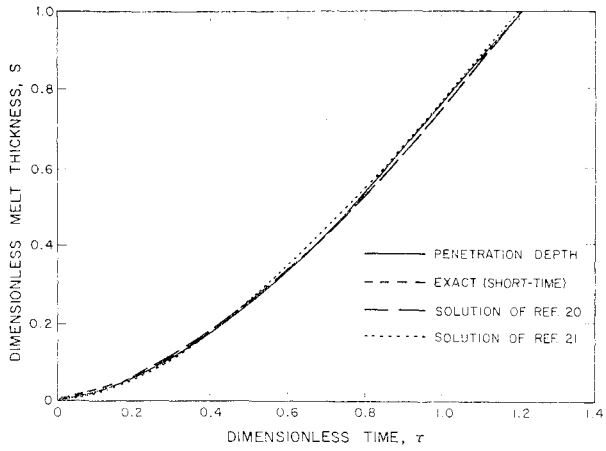

Fig. 2 Propagation of melt surface.

follows:

$$\theta(y,\tau) = \begin{cases} 1 - \bar{Q}\left[1 - 2\tau - \dfrac{2\bar{Q}^2 - 3\bar{Q} + 1}{3\bar{Q}^2}\right] + \\ \bar{Q}(1-S)^2(1-y)^2 + \bar{Q}\left[1 - 2\tau - \right. \\ \left. (1-S)^2 - \dfrac{2\bar{Q}^2 - 3\bar{Q} + 1}{3\bar{Q}^2}\right]\left(1 - \dfrac{y}{q_1}\right)^2 & (25) \\ 0 < y < q_1 \\ 1 - \bar{Q}\left[1 - 2\tau - \dfrac{2\bar{Q}^2 - 3\bar{Q} + 1}{3\bar{Q}^2}\right] + \\ \bar{Q}(1-S)^2(1-y)^2 \qquad q_1 < y < 1 \end{cases}$$

Substitution of this solution into Eqs. (13) and (7b) again results in two simultaneous equations whose solution yields $S(\tau)$ and $q_1(\tau)$. These equations are given in Table 1, and yield, for large $\bar{Q}\mu$,

$$\tau_{q_1=1} = (-\bar{Q}^2 + 6\bar{Q} - 2)/(12\bar{Q}^2) \tag{26}$$

For the heating range $\bar{Q} > 2$, Eqs. (22–23) are valid in $0 \leq \tau \leq \tau_E$, or until the disturbance due to melting catches up with that due to heating. Again, for large μ, τ_E can be shown to be

$$\tau_E = 1/(2\bar{Q}^2) \tag{27}$$

Beyond this time, only one penetration depth, denoted by q_1, exists, and the region $q_1 < y < 1$ remains unheated. In $\tau_E \leq \tau \leq \tau_{q_1=1}$, a solution satisfying the same conditions as those of the case for which $1 < \bar{Q} < 2$, is

$$\theta(y,\tau) = \begin{cases} (1 - y/q_1)^2 & 0 < y < q_1 \\ 0 & q_1 < y < 1 \end{cases} \tag{28}$$

The equations necessary to solve for $S(\tau)$ and $q_1(\tau)$ are presented in Table 1, and result in

$$\tau_{q_1=1} = (\bar{Q} - 1)/(2\bar{Q}) \tag{29}$$

for large values of $\bar{Q}\mu$.

In $\tau_{q_1=1} \leq \tau \leq \tau^*$, the solution for all $\bar{Q} > 1$ is

$$\theta(y,\tau) = 1 - \bar{Q}F(\tau) + \bar{Q}F(\tau)(1-y)^2 \qquad 0 < y < 1 \tag{30}$$

This solution is continuous with that of Eqs. (25) and (28) for $1 < \bar{Q} < 2$ and $\bar{Q} > 2$, respectively, and satisfies all three boundary conditions (5a–5c) identically. Substitution of Eq. (30), which is identical to that of Eq. (21) for $0 < \bar{Q} \leq 1$, into the overall heat balance of Eq. (13) results in a differential equation for $S(\tau)$ which is different from that for the lower heating range only because the expressions for τ_m are not of the same form. The equation for $S(\tau)$ in this time range is found in Table 1.

Comparison of Solution with Exact Short-Time Solution and Other Approximate Solutions

The accuracy of the present solution is measured by comparison with the results of two other approximate methods[20,21] and with the known exact short-time solution. The latter is given in Ref. 18 and is derived by use of Boley's embedding technique.[10] Neither this exact solution nor those obtained from the methods of Refs. 20 and 21 will be repeated. It suffices, for our present purposes, to present comparisons of the results of the various approximate methods with each other and with the exact short-time solution. This is done in Figs. 2 and 3.

The propagation of the melt surface as computed by use of each of the three approximate methods is shown in Fig. 2 for $\bar{Q} = 0.25$ and $\mu = 2.25$. The exact solution is also plotted on this figure for short postmelting times. It is seen that all three approximate solutions are in good agreement with the exact solution for short times, and with each other over the entire melting period. Curves of temperature vs time are presented in Fig. 3 for various surfaces x/h. It is clear that the use of the present approximate method results in a solution that is in good agreement with the exact solution for short melting times, and appears to be physically more reliable than that obtained using the method of Ref. 20.

Temperature Solution upon Removal of Heat Pulse

It has been shown that, upon removal of the heat pulse at $\tau = \tau^*$, no further melting will occur.[18] Thus, for $\tau > \tau^*$, the problem to be solved is that of a plate of constant thickness, insulated at both faces, and subjected to an initial temperature distribution. At this time, it is convenient to introduce the reduced dimensionless time variable

$$\bar{\tau} = (\tau - \tau^*)/[1 - S(\tau^*)]^2 \tag{31}$$

Assuming for simplicity, but without loss of generality, that $\tau_{q_1=1} < \tau^* < \tau_h$, the heat conduction equation, and initial and boundary conditions in dimensionless form are as follows:

$$\frac{\partial^2\theta}{\partial y^2} - \frac{\partial\theta}{\partial\bar{\tau}} = 0; \qquad 0 < y < 1 \qquad \bar{\tau} > 0 \tag{32}$$

$$\frac{\partial\theta}{\partial y} = 0; \qquad y = 0 \qquad \bar{\tau} > 0 \tag{33a}$$

$$\frac{\partial\theta}{\partial y} = 0; \qquad y = 1 \qquad \bar{\tau} > 0 \tag{33b}$$

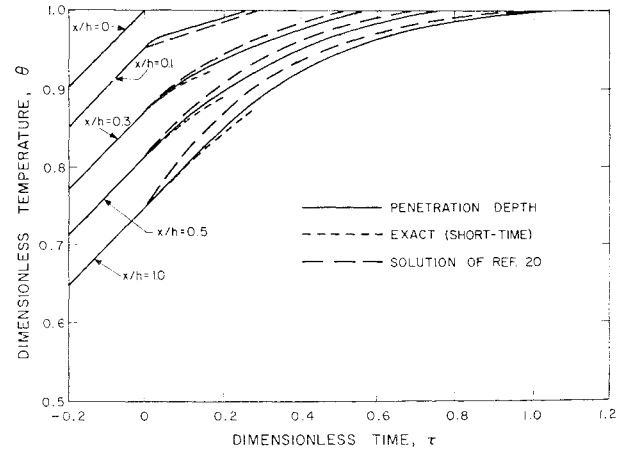

Fig. 3 Typical temperature history.

$$\theta = 1 - \bar{Q}F(\tau^*) + \bar{Q}F(\tau^*)(1 - y)^2; \qquad 0 < y < 1 \qquad \bar{\tau} = 0 \quad (33c)$$

The solution to this set of equations is similar to that in the premelting regime, and, with $F(\tau^*) = F^*$, is given by

$$\theta(y,\bar{\tau}) = \begin{cases} 1 - \bar{Q}F^* + \bar{Q}F^*(1 - y)^2 + \frac{1}{3}\bar{Q}F^*q_2^2 - \\ \qquad \bar{Q}F^*q_2(1 - y/q_2)^2; \quad 0 < y < q_2 \\ 1 - \bar{Q}F^* + \bar{Q}F^*(1 - y)^2 + \frac{1}{3}\bar{Q}F^*q_2^2; \\ \qquad q_2 < y < 1 \end{cases} \quad (34)$$

This solution satisfies Eqs. (33a–33c) and the over-all heat balance which, in a manner identical to that used during the heating period, is obtained as

$$\int_0^1 \theta(y,\bar{\tau})dy = \int_0^1 \theta(y,0)dy = 1 - \frac{2}{3}\bar{Q}F^* \quad (35)$$

A solution satisfying Eq. (30) in $0 < y < q_2$ identically is obtained when

$$q_2(\bar{\tau}) = [6\bar{\tau}]^{1/2} \quad (36)$$

What can be considered as a steady state condition is attained when $q_2 = 1$, at which time ($\bar{\tau} = \bar{\tau}_{q_2=1}$) the temperature is uniform throughout the plate. It is easily seen that

$$\bar{\tau}_{q_2=1} = \tfrac{1}{6} \quad (36a)$$

and, for $\bar{\tau} = \frac{1}{6}$,

$$\theta(y,\bar{\tau}) = 1 - \tfrac{2}{3}\bar{Q}F^* \quad (37)$$

Solutions for Melt Thickness and Penetration Depth

Equations necessary to solve for the melt thickness $S(\tau)$, and the penetration depth due to melting $q_1(\tau)$, are given in Table 1 for all heating ranges. In each set of equations, which are all nonlinear, is one first-order differential equation, while the remaining, if any, are algebraic equations. To eliminate the necessity for the solution of these equations in rapid design calculations, approximate, explicit expressions for $S(\tau)$ and $F(\tau)$ are given, the latter being used to calculate the melting rate $\dot{S}(\tau)$. Once these two equations are evaluated at a given time, it is an easy matter to compute the penetration depth, if one exists, at that time directly from the equations.

If more accurate solutions are desired, it is necessary to integrate numerically the equations in Table 1. This can be done with little difficulty by approximating the only derivative present $\dot{S}(\tau)$, by using the first central difference of $S(\tau)$, and employing a starting solution in the neighborhood of $\tau = 0$ obtained from the tabulated equations.

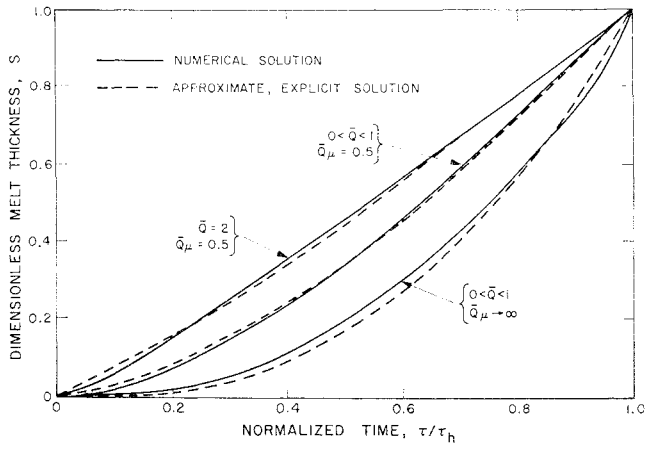

Fig. 4 Melt thickness—numerical and explicit solutions.

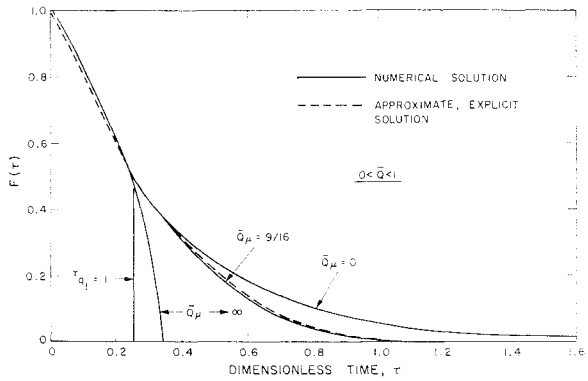

Fig. 5 $F(\tau)$—numerical and explicit solutions.

Comparisons of results obtained by using the explicit expressions for $S(\tau)$ and $F(\tau)$, with those obtained by numerically integrating the pertinent equations, are illustrated in Figs. 4 and 5, respectively. The typical plots of $S(\tau)$ vs τ and $F(\tau)$ vs τ indicate that the approximate explicit results are in good agreement with those evaluated numerically for all melting times. Further numerical results supporting these conclusions for other values of the parameters are found in Ref. 18.

Stresses and Deformations

The calculation of stresses and deformations in a melting plate is carried out on the basis of the material behaving as a homogeneous, isotropic, elastic-perfectly plastic solid. Its elastic properties (E and ν) are taken to be constant, the thermal expansion is linear, and the uniaxial yield stress Y, varies linearly with temperature in accordance with Eq. (1). The yield criterion used is that of von Mises, given in Eq. (2).

The development of the formulation for the mechanical response of a thin, flat, elastic-plastic plate subjected to a transient one-dimensional temperature field through the thickness is presented in detail in Boley and Weiner.[9] The resultant stress and strain fields are found to be isotropic and uniform in the plane of the plate and vary only through the thickness. This simplification is valid for a plate of arbitrary planform provided no mechanical loads act on the plate (free plate). The validity is maintained, however, for a mechanically loaded simply supported plate provided 1) the plate is circular, 2) there is edge loading only (no surface loading), and 3) the loading is axisymmetric. Though the formulation was derived there[9] for a plate with nonmoving boundaries, its extension to a melting plate is apparent.

The only nonzero stress components are the normal stresses in the plane of the plate. In fact, since the stress field in this plane is isotropic and uniform, there remains just one independent unknown stress component to be calculated. Denoting this component by $\sigma(x,t)$, the yield criterion of Eq. (2) becomes

$$f = (\sigma^2 - Y^2)/3 = 0 \quad (38)$$

and the general expression for the stress rate is

$$\dot{\sigma}(x,t) = g(x,t)\,[E/(1 - \nu)]\,[\dot{\epsilon}(x,t) - \alpha\dot{T}(x,t)] + [1 - g(x,t)](\mathrm{sgn}\sigma)\dot{Y}[T(x,t)] \quad (39)$$

In Eq. (39), $\epsilon(x,t)$ is the in-plane strain corresponding to $\sigma(x,t)$, sgn $\sigma = 1$ if $\sigma > 0$, or -1 if $\sigma < 0$ (sgnσ thus specifies whether a plastic region is in a tensile or compressive state), and

$$g(x,t) = 1 \text{ if } f < 0, \text{ or if } f = 0 \text{ and } \dot{f} < 0$$
$$g(x,t) = 0 \text{ if } f = 0 \text{ and } \dot{f} = 0 \quad (40)$$

These three possible combinations of f and $\dot{f}$ represent, respectively, an elastic state of stress, elastic unloading from a previously plastic state of stress, and continuation of plastic flow.

For typical conditions of atmospheric re-entry, it is reasonable to assume that thermal and mechanical loads build up steadily in the same time period (loading) and then, after the attainment of peak values, decrease simultaneously (unloading). For the purposes of the calculations in this paper, it is hypothesized that thermal loading and mechanical loading peak simultaneously. This is an idealization that greatly facilitates the formulation and solution of the problem. Because of the steadily increasing thermal and mechanical loads, it is assumed that all plastic regions initiated in the plate during the loading period undergo steady increases in thickness until the time of peak loading. In the present case, this time is the time at which the heat pulse is removed, $t = t^*$. Thus, the calculation of the mechanical response during loading ($0 < t < t^*$) is considered separately from that during unloading ($t > t^*$).

Stresses and Deformations During Loading

Consider the plate to be unstressed and undeformed at $t = 0$. Since there is no unloading in $0 < t < t^*$, Eq. (39) may be integrated directly to give

$$\sigma(x,t) = g(x,t)[E/(1-\nu)][\epsilon(x,t) - \alpha T(x,t)] + [1 - g(x,t)](\mathrm{sgn}\sigma)Y[T(x,t)] \quad (41)$$

where

$$g(x,t) = 1 \text{ if } \sigma^2 < Y^2,\ g(x,t) = 0 \text{ if } \sigma^2 = Y^2 \quad (42)$$

$g(x,t)$ and $\epsilon(x,t)$ are the two unknown functions whose solutions yield the stresses and deformations in $0 < t < t^*$. These functions are evaluated by making use of the equations of compatibility and the edge boundary conditions.

The two compatibility equations that are not satisfied identically reduce to the same equation for $\epsilon(x,t)$

$$\partial^2\epsilon(x,t)/\partial x^2 = 0 \quad (43)$$

This results in

$$\epsilon(x,t) = F_1(t) + F_2(t)x \quad (44)$$

The edge conditions are in the form:

$$\int_{s(t)}^{h} \sigma(x,t)dx = N(t),\ \int_{s(t)}^{h} \sigma(x,t)[x - s(t)]dx = M(t) \quad (45)$$

where $N(t)$ and $M(t)$ are the prescribed axisymmetric resultant edge force and resultant edge moment, respectively, with the latter taken about the melt surface $x = s(t)$. Since there are no variations of stress in the plane of the plate, Eq. (45) is valid throughout the plate except, according to Saint Venant's principle, in the immediate vicinity of the edge.

In addition to the dimensionless variables and parameters of Eqs. (5) and (8), the following dimensionless notation is convenient:

$$\bar{\sigma}(y,\tau) = \frac{\sigma(x,t)}{Y_0};\quad \bar{Y}(y,\tau) = \frac{Y(x,t)}{Y_0} = 1 - \theta(y,\tau);\quad \beta = \frac{\alpha E T_m}{(1-\nu)Y_0}$$

$$C_1(\tau) = \frac{E}{(1-\nu)Y_0}[F_1(t) + F_2(t)s(t)];\quad C_2(\tau) = \frac{E}{(1-\nu)Y_0}F_2(t)[h - s(t)] \quad (46)$$

With Eqs. (44) and (46), Eq. (41) becomes**

$$\bar{\sigma}(y,\tau) = g(y,\tau)[-\beta\theta(y,\tau) + C_1(\tau) + C_2(\tau)y] + [1 - g(y,\tau)](\mathrm{sgn}\bar{\sigma})[1 - \theta(y,\tau)] \quad (47)$$

where

$$g = 1 \text{ if } |\bar{\sigma} < 1 - \theta,\ g = 0 \text{ if } \bar{\sigma} = 1 - \theta \quad (48)$$

$C_1(\tau)$ and $C_2(\tau)$ are found by substituting Eq. (47) into each of the boundary conditions (45) which, in dimensionless form, are

$$\int_0^1 \bar{\sigma}(y,\tau)dy = \bar{N}(\tau),\ \int_0^1 \bar{\sigma}(y,\tau)ydy = \bar{M}(\tau) \quad (49)$$

where $\bar{N}(\tau)$ and $\bar{M}(\tau)$ are dimensionless edge loads defined by

$$\bar{N}(\tau) = N(t)/\{Y_0[h - s(t)]\} = N/[Y_0h(1-S)]$$
$$\bar{M}(\tau) = M(t)/\{Y_0[h - s(t)]^2\} = M/[Y_0h^2(1-S)^2] \quad (50)$$

The locations of the interfaces between the elastic and plastic regions are found, and thus the function $g(y,\tau)$ is determined, by requiring continuity of stress at each of the interfaces y_i. This results in equations of the following type:

$$-\beta\theta(y_i,\tau) + C_1(\tau) + C_2(\tau)y_i = \pm[1 - \theta(y_i,\tau)] \quad (51)$$

The simultaneous solution of Eqs. (49) yields the values of C_1 and C_2.

The plate deformations are determined directly from the in-plane strain $\epsilon(x,t)$, which, in turn, is completely determined by C_1 and C_2 [see Eqs. (44) and (46)]. For a thin, circular plate of radius R (see Fig. 1), the radial edge displacement u, and the maximum transverse deflection w (at the center of the plate), are given by

$$u = u_0(C_1 + C_2y) \quad (52)$$

$$w = w_0C_2/(1-S) \quad (53)$$

where

$$u_0 = [(1-\nu)hY_0/E](R/h);\quad w_0 = [(1-\nu)hY_0/(2E)](R/h)^2 \quad (54)$$

Before considering the numerical solution of a particular problem, it is useful to see whether some general conclusions about the nature of the mechanical response can be obtained. For an edge-loaded plate, unfortunately, this is difficult to do since the formation of the plastic regions is very strongly dependent on the intensities, signs, and time variations of the mechanical loading terms $\bar{N}(\tau)$, and $\bar{M}(\tau)$, as well as on the heat input and the material properties. For this reason, the growth history of plastic regions in an edge-loaded plate is examined only in an illustrative example. With regard to a free plate, on the other hand, some general properties of the stress history can be stated for the case in which the heat input is a square pulse.

For a plate of arbitrary planform in which $\bar{N} = \bar{M} = 0$, one, two, or three plastic regions may exist at a given time, as follows:

1) Since the plate is initially ($t = 0$) stress free, the stress distribution for short premelting times is elastic; it is also symmetric about the midplane of the plate. Since the yield stress at melting is zero, plastic flow must commence prior to the time of initial melting ($t = t_m$). The first plastic region is initiated in compression at the heated surface $y = 0$, because the temperature is a maximum and hence the yield stress a minimum, at this surface. If the material parameter β is such that $\beta < 8.48$ [corresponding to relatively high yield

** The formulas which follow are applicable to simply supported beams merely by letting $\beta = \alpha ET_m/Y_0$, $C_1 = E(F_1 + F_2s)/Y_0$, and $C_2 = EF_2(h - s)/Y_0$.

stresses—see Eq. (46)], only one plastic region, adjacent to the surface $y = 0$, exists throughout the loading period.

2) If $\beta > 8.48$, a second plastic region is initiated in compression at the insulated surface $y = 1$. If $0 < \bar{Q} \leq 1$, this region is initiated prior to the onset of melting while, for $\bar{Q} > 1$, this may occur either before or after $t = t_m$. No more than two plastic regions exist during the entire loading period if $\beta < 18$.

3) A third plastic region is initiated in tension at some internal surface only if $\beta > 18$. Again, this will occur before, or either before or after, the onset of melting, according to whether $0 < \bar{Q} \leq 1$ or $\bar{Q} > 1$, respectively.

The present results can be used to study the use of thermoelastic stress analyses for plastic structures subject to high thermal gradients. It has been stated that total deformations computed by including the effects of plastic flow differ little from elastically computed deformations (see, for example, Refs. 16 and 17). The accuracy of this statement for the melting plate can be seen by referring to Fig. 6, in which $C_1(\tau)$ and $C_2(\tau)$, the two functions that completely determine the deformation history, are plotted against time for typical values of the thermal parameters $\bar{Q} = 0.25$ and $\mu = 2.25$, and for values of $\beta = 5$ and 10. Plots are presented for both elastic-plastic and elastic solutions, for the case in which loading continues until the entire plate is melted (i.e., $t_h < t^*$). It is seen that the elastic solutions yield fairly good upper bounds to the corresponding elastic-plastic solutions during loading. The results of an illustrative problem to be presented subsequently, lead to the same conclusion in both the loading and unloading periods. On the basis of these results, one may expect that a thermoelastic analysis will yield a deformation history that is conservative for design purposes, and not too greatly in error.

Stresses and Deformations During Unloading

It was shown previously that, upon removal of the heat pulse at $t = t^*$, a decrease of temperature gradients results until the temperature distribution through the plate becomes uniform. This, in turn, gives rise to stress unloading which, for an elastic-plastic plate, leads to the existence of residual stresses and deformations.

A surface at any depth (defined by y), existing in a plastic state of stress ($f = 0$) at $t = t^*$ continues to respond in one of two ways [see Eqs. (40)]:

1) Continuation of plastic flow in which the yield stress varies with temperature. This occurs when $\dot{f} = 0$.

2) Elastic unloading taking place when $\dot{f} < 0$. From Eqs. (38, 39, and 46), this may be shown to be equivalent to

$$(\text{sgn}\sigma)(-\beta\dot{\theta} + \dot{C}_1 + \dot{C}_2 y) + \dot{\theta} < 0 \qquad (55)$$

It will now be demonstrated that the idealization of assuming all surfaces in a plastic state of stress at $t = t^*$ to be simultaneously unloaded elastically at this time, gives results

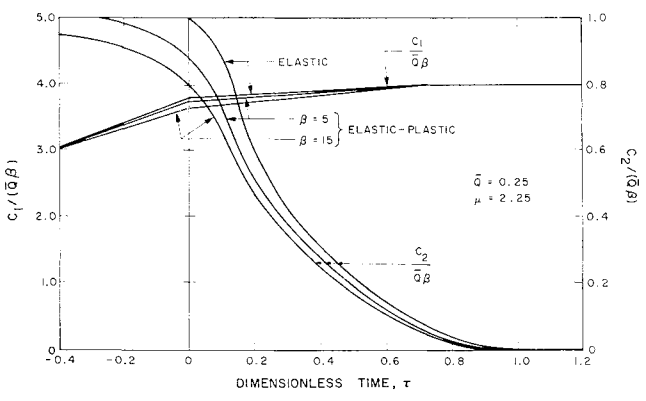

Fig. 6 Deformation functions for melting plate.

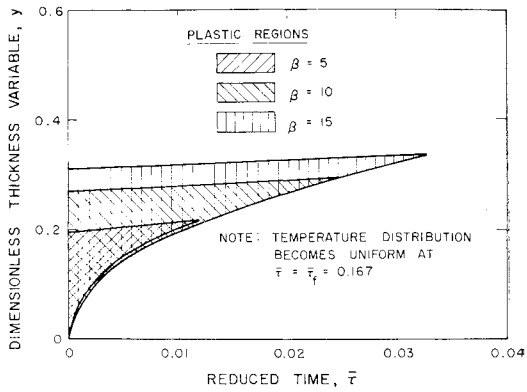

Fig. 7 Unloading of plastic regions.

which are in good agreement with those obtained using the exact, rather complex analysis which includes elastic unloading and continuation of plastic flow. For each region not simultaneously unloaded elastically, the latter analysis gives rise to elastic unloading such that the thickness of the plastic region decreases continuously until unloading is complete (i.e., temperature distribution through the plate thickness is uniform). This is henceforth referred to as continuous elastic unloading.

Thus, two analyses—namely those of continuous and simultaneous elastic unloading—are carried out here for a free plate; again, for edge-loaded plates, only solutions of specific problems will be practicable. For purposes of clarity in interpreting results, but without loss of generality, the removal of the heat pulse is taken to occur after the postmelting transit time (i.e., $\tau^* > \tau_{q_1=1}$). The temperature distributions during unloading are therefore given by Eqs. (34), regardless of the numerical values of $\bar{Q}$ and μ. The results of the two analyses follow.

Continuous elastic unloading

This analysis is carried out based on elastic unloading occurring only at those surfaces where $f = 0$ and $\dot{f} < 0$. Since elastic unloading of all previously plastic surfaces does not occur at the same time, the calculation of stress distributions and deformations during the unloading period must be executed using the general expression for stress rates of Eq. (39), followed by step-by-step integration of the rates. Hence, it is seen that the complexity of the solution arises from the dependence on the past history of stresses and deformations. The solution is obtained by numerical means,[18] and results in simultaneous elastic unloading in all plastic regions at $t = t^*$, except in that region adjacent to the surface $y = 0$. This holds regardless of the number of plastic regions existing at this time; i.e., regardless of the value of β.

The unloading process in the region adjacent to $y = 0$ is shown in Fig. 7, for $\beta = 5$, 10, and 15. It is seen that in all three cases, completion of elastic unloading in this region is attained well before the time at which the temperature distribution becomes uniform. The significance of this observation will be discussed shortly.

Simultaneous elastic unloading

Simultaneous elastic unloading at $t = t^*(\bar{\tau} = 0)$ implies that changes in the stress distribution throughout the plate during the entire unloading period are elastic, unless, of course, reversal of stress is of sufficient magnitude to result in the formation of new plastic regions. The equation for stress during unloading, valid in any region in which plastic flow has not occurred as a result of stress reversal (i.e., any

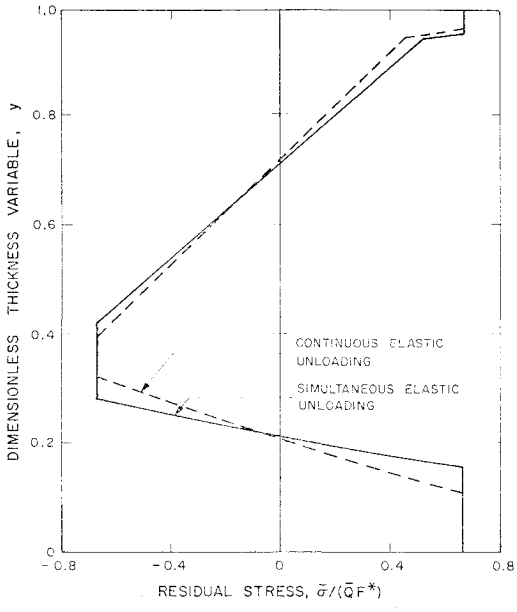

Fig. 8 Residual stress distribution; $\beta = 15$.

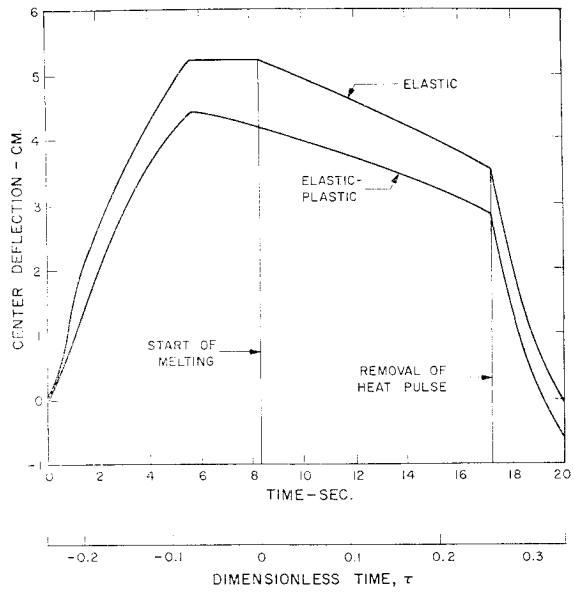

Fig. 10 Deflection of a melting circular plate.

r region in which $|\bar{\sigma}| < \bar{Y} = 1 - \theta$), is then given by

$$\bar{\sigma}(y,\bar{\tau}) = \bar{\sigma}(y,0) - \beta[\theta(y,\bar{\tau}) - \theta(y,0)] + [C_1(\bar{\tau}) - C_1(0)] + [C_2(\bar{\tau}) - C_2(0)]y \quad (56)$$

If yielding has occurred,

$$\bar{\sigma}(y,\bar{\tau}) = (\text{sgn}\bar{\sigma})[1 - \theta(y,\bar{\tau})] \quad (57)$$

The values of $C_1(\bar{\tau})$ and $C_2(\bar{\tau})$ are found by satisfying the boundary conditions [Eqs. (49)]. The locations of the interfaces, if any, between the elastic and plastic regions are determined by requiring the stress to be continuous throughout the plate.

The outstanding advantage of the simultaneous elastic unloading idealization is that the stress distribution at any time during the unloading period may be found without knowledge of the mechanical response at any previous time, except, of course, at the time of initial unloading, $\bar{\tau} = 0$. This yields explicit expressions for stresses [Eqs. (56) and (57)], and thus avoids the need for using a complex numerical scheme to obtain the solution.

The accuracy of this simplified approach may be judged by referring to Fig. 8, in which residual stress distributions for a typical value of $\beta(\beta = 15)$ are plotted for both the continuous and simultaneous elastic unloading analyses, and can be seen to be in reasonable agreement with each other. The physical reason for this is that, in the case of continuous elastic unloading, all elastic unloading, though not occurring simultaneously at $\bar{\tau} = 0$, is accomplished within a relatively short time after $\bar{\tau} = 0$; beyond this time, unloading is elastic in both cases unless new plastic regions are formed.

With respect to the nature of the residual stress distribution, it is found that, for the case of simultaneous elastic unloading, this distribution is elastic if $0 < \beta < 4$, or elastic-plastic with one, two, or three plastic regions being formed during unloading if $4 < \beta < 10.94$, $10.94 < \beta < 11.28$, or $\beta > 11.28$, respectively. Sketches of typical stress distributions at the time of removal of the heat pulse $\bar{\tau} = 0$, and at the time of uniform temperature $\bar{\tau} = \bar{\tau}_f$ (residual stress distributions), are presented in Fig. 9 for all ranges of β. Yield stress distributions, which bound the stress distributions, are given by dashed lines.

Illustrative Example

For illustrative purposes, the material properties, thickness, and heating history of the steel plate used in Ref. 12 are employed. The plate is subjected to thermal loading as would result from atmospheric re-entry, in which the total heat input is 2244 cal/cm², and the total thickness of melted material is three-tenths that of the original plate thickness.

It is therefore desired to find a heat pulse such that the total heat input and the amount of melted material are the

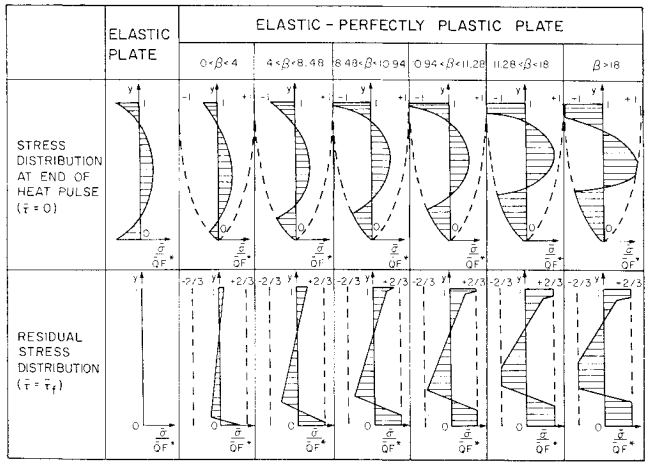

Fig. 9 Typical stress distributions.

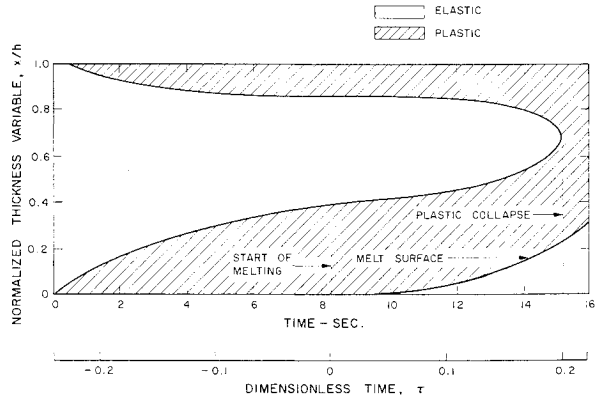

Fig. 11 Growth of plastic regions in edge-loaded plate.

same as those encountered in Ref. 12; i.e.,

$$\int_0^{t^*} Q(t)dt = 2244 \text{ cal/cm}^2$$

and $s(t^*)/h = S(\tau^*) = 0.3$. The heat pulse satisfying these criteria is defined by $Q_0 = 131$ cal/cm^2/sec and $t^* = 17.2$ sec [see Eq. (4)]. The material properties of the plate give $\mu = 22.5$ and $\beta = 15$ for the dimensionless material parameters, and $\bar{Q} = 0.87$ for the dimensionless heat input [see Eqs. (8) and (46)].

Typical results are presented describing the stress and deformation history of a free plate, and the growth of plastic regions in an edge-loaded plate.

For the free plate, it is seen from Fig. 9 that, since $\beta = 15$, two plastic regions are formed during loading and three plastic regions exist in the residual stress distribution. The deformation history is such that for a circular plate of radius $R = 40$ cm, the average residual edge expansion and maximum residual deflection (at the center of the plate) are 0.426 cm and -0.533 cm, respectively. If the plate were perfectly elastic, these values would be 0.434 cm and zero, respectively; the former is due solely to thermal expansion and the latter to the absence of thermal bending in a uniformly heated, elastic plate.

A plot of center deflection against time is presented in Fig. 10 for both an elastic-perfectly plastic and a perfectly elastic plate. It is seen that, in both cases, the maximum deflection is attained before the onset of melting. The elastic solution is also seen to give an upper bound to the elastic-plastic solution throughout the entire process (loading and unloading).

For a plate subjected to the constant dimensionless edge loads $\bar{N} = -0.35$ and $\bar{M} = -0.22$, the growth of the two compressive plastic regions is shown in Fig. 11. It is seen that at $t = 15.2$ sec ($\tau = 0.20$), the entire plate is in a plastic state of stress, which indicates plastic collapse—a phenomenon that cannot occur in a plate free of edge loads but which is of obvious importance in the mechanical design of a melting plate.

References

[1] Boley, B. A., "The Analysis of Problems of Heat Conduction and Melting," *High Temperature Structures and Materials: Proceedings of the Third Symposium on Naval Structural Mechanics*, Pergamon Press, New York, 1964, pp. 260–315.

[2] Muehlbauer, J. C. and Sunderland, J. E., "Heat Conduction with Freezing or Melting," *Applied Mechanics Reviews*, Vol. 18, No. 12, Dec. 1965, pp. 951–959.

[3] Goodman, T. R., "Application of Integral Methods to Transient Non-linear Heat Transfer," *Advances in Heat Transfer*, Vol. 1, Academic Press, New York, 1964, pp. 51–122.

[4] Rogers, T. G. and Lee, E. H., "Thermo-Viscoelastic Stresses in a Sphere with an Ablating Cavity," TR 6, Contract NOrd-18594, Aug. 1962, Brown Univ.

[5] Sternberg, E. and Gurtin, M. E., "Uniqueness in the Theory of Thermo-Rheologically Simple Ablating Viscoelastic Solids," TR No. 16, Contract Nonr-262-(25), Sept. 1962, Brown Univ.

[6] Weiner, J. H. and Boley, B. A., "Elasto-Plastic Thermal Stresses in a Solidifying Body," *Journal of the Mechanics and Physics of Solids*, Vol. 11, 1963, pp. 145–154.

[7] Schuyler, F. L. and Friedman, E., "High Temperature Ablation Interaction," *Mechanics of Composite Materials: Proceedings of the Fifth Symposium on Naval Structural Mechanics*, Pergamon Press, New York, 1970, pp. 769–798.

[8] Tadjbakhsh, E., "Thermal Stresses in an Elastic Half-Space with a Moving Boundary," Research Report RC-616, Jan. 1962, IBM; also *AIAA Journal*, Vol. 1, No. 1, Jan. 1963, pp. 214–215.

[9] Boley, B. A. and Weiner, J. H., *Theory of Thermal Stresses*, Wiley, New York, 1960, Chap. 6.

[10] Boley, B. A., "A Method of Heat Conduction Analysis of Melting and Solidification Problems," *Journal of Mathematics and Physics*, Vol. 40, No. 4, Dec. 1961, pp. 300–313.

[11] Wu, T. S. and Boley, B. A., "Bounds in Melting Problems with Arbitrary Rates of Liquid Removal," *SIAM Journal*, Vol. 14, No. 2, March 1966, pp. 306–323.

[12] Citron, S. J., "Heat Conduction in a Melting Slab," *Journal of the Aerospace Sciences*, Vol. 27, No. 3, March 1960, pp. 219–228.

[13] Goodman, T. R., "Aerodynamic Ablation of Melting Bodies," *Proceedings of the Third U.S. National Congress of Applied Mechanics*, June 1958.

[14] Sutton, G. W., "The Hydrodynamics and Heat Conduction of a Melting Surface," *Journal of the Aerospace Sciences*, Vol. 25, No. 1, Jan. 1958, pp. 29–32.

[15] Hoff, N. J., "Structures and Materials for Finite Lifetime," *Advances in Aeronautical Sciences*, Vol. 2, Pergamon Press, New York, 1958.

[16] Mendelson, A. and Manson, S. S., "Practical Solution of Plastic Deformation Problems in Elastic-Plastic Range," TN 4088, Sept. 1957, NACA.

[17] Mendelson, A., *Plasticity: Theory and Application*, MacMillan, New York, 1968.

[18] Friedman, E. and Boley, B. A., "Design Estimates of Stresses and Deformations in Melting Plates," TR 29, Contract Nonr-4259(07), June 1965, Dept. of Civil Engineering and Engineering Mechanics, Columbia Univ.

[19] Biot, M. A., "New Methods in Heat Flow Analysis with Application to Flight Structures," *Journal of the Aeronautical Sciences*, Vol. 24, No. 12, Dec. 1957, pp. 857–873.

[20] Goodman, T. R. and Shea, J. J., "The Melting of Finite Slabs," *Journal of Applied Mechanics*, Vol. 27, No. 1, March 1960, pp. 16–24.

[21] Citron, S. J., "On the Conduction of Heat in a Melting Slab," *Proceedings of the Fourth U.S. National Congress of Applied Mechanics*, June 1962, pp. 1221–1227.